

Title	Influence of carrier confinement on the subthreshold swing of multigate silicon-on-insulator transistors
Authors	Colinge, Jean-Pierre;Afzalian, Aryan;Lee, Chi-Woo;Yan, Ran;Akhavan, Nima Dehdashti
Publication date	2008
Original Citation	Colinge, J.-P., Afzalian, A., Lee, C.-W., Yan, R. and Akhavan, N. D. (2008) 'Influence of carrier confinement on the subthreshold swing of multigate silicon-on-insulator transistors', Applied Physics Letters, 92(13), pp. 133511. doi: 10.1063/1.2907330
Type of publication	Article (peer-reviewed)
Link to publisher's version	<a href="http://aip.scitation.org/doi/abs/10.1063/1.2907330">http://aip.scitation.org/doi/abs/10.1063/1.2907330</a> - 10.1063/1.2907330
Rights	© 2008 American Institute of Physics. This article may be downloaded for personal use only. Any other use requires prior permission of the author and AIP Publishing. The following article appeared in Colinge, J.-P., Afzalian, A., Lee, C.-W., Yan, R. and Akhavan, N. D. (2008) 'Influence of carrier confinement on the subthreshold swing of multigate silicon-on-insulator transistors', Applied Physics Letters, 92(13), pp. 133511 and may be found at <a href="http://aip.scitation.org/doi/abs/10.1063/1.2907330">http://aip.scitation.org/doi/abs/10.1063/1.2907330</a>
Download date	2025-01-25 01:56:04
Item downloaded from	<a href="https://hdl.handle.net/10468/4371">https://hdl.handle.net/10468/4371</a>



# UCC

**University College Cork, Ireland**  
Coláiste na hOllscoile Corcaigh

# Influence of carrier confinement on the subthreshold swing of multigate silicon-on-insulator transistors

Jean-Pierre Colinge, Aryan Afzalian, Chi-Woo Lee, Ran Yan, and Nima Dehdashti Akhavan

Citation: *Appl. Phys. Lett.* **92**, 133511 (2008); doi: 10.1063/1.2907330

View online: <http://dx.doi.org/10.1063/1.2907330>

View Table of Contents: <http://aip.scitation.org/toc/apl/92/13>

Published by the [American Institute of Physics](#)

---

---



*CiSE* magazine is  
an innovative blend.

## Influence of carrier confinement on the subthreshold swing of multigate silicon-on-insulator transistors

Jean-Pierre Colinge,<sup>a)</sup> Aryan Afzalian, Chi-Woo Lee, Ran Yan, and Nima Dehdashti Akhavan

Tyndall National Institute, University College Cork Lee Maltings, Prospect Row, Cork, Ireland

(Received 26 February 2008; accepted 17 March 2008; published online 3 April 2008)

The minimum energy of the first conduction subband varies with gate voltage in trigate silicon-on-insulator metal-oxide-silicon field-effect transistors (MOSFETs) in subthreshold operation. In an inversion-mode trigate device, the energy level of the lowest subband increases with electron concentration, while it decreases under the same conditions in some accumulation-mode devices. As a result of this quantum effect, the subthreshold swing of accumulation-mode trigate FETs is smaller than predicted by classical theory. This effect is not observed in fin-shaped FETs and gate-all-around MOSFETs and can be amplified by modifying the device cross section. © 2008 American Institute of Physics. [DOI: 10.1063/1.2907330]

It is well known that the energy of the conduction subbands increases in trigate field-effect transistors (FETs) when the section of the device is reduced. This effect is similar to the increase of subband energy in ultrathin silicon-on-insulator (SOI) metal-oxide-silicon (MOSFETs) when the silicon film thickness is reduced below 10 nm.<sup>1-5</sup> Furthermore, in inversion-mode (IM) devices, the minimum energy of the energy subbands increases when the electron concentration is increased, which dynamically increases the threshold voltage as the inversion charge builds up. This effect reduces the current drive of the device and is not predicted by classical simulators. It also increases the value of the subthreshold swing, expressed in millivolts per decade, as the energy of the first subband increases with carrier concentration in subthreshold operation.<sup>6</sup> In this paper, we analyze this phenomenon in different type of multigate SOI devices operating either in inversion or accumulation mode.

Two-dimensional simulations of fin-shaped FETs (FinFETs), trigate and gate-all-around FETs (GAA FETs) have been carried out by self-consistently solving the Poisson equation and the Schrödinger equation.<sup>6</sup> The devices are *N* channel and both IM operation and accumulation-mode (AM) operation were simulated. The gate oxide thickness  $t_{\text{ox}}$ , is 2 nm and the buried oxide thickness  $t_{\text{BOX}}$  is 10 nm. The fin height or silicon film thickness  $t_{\text{Si}}$  is equal to the device width  $W_{\text{Si}}$  in the trigate and GAA devices, and it is equal to  $3 \times W_{\text{Si}}$  in the FinFETs. There is no hard mask at the top of the FinFET, which, therefore, basically behaves as a trigate FET with a 3:1 height-to-width aspect ratio. The IM devices have a *p*-type doping concentration of  $5 \times 10^{18} \text{ cm}^{-3}$  and the AM devices an *n*-type doping concentration of  $2 \times 10^{19} \text{ cm}^{-3}$ . Such a large doping concentration is necessary to allow for some “bulk” current flow devices with such small cross sections. The devices can, however, be turned off by applying a sufficiently negative gate voltage.

Devices with a larger section ( $10 \times 10 \text{ nm}^2$  for GAA and trigate devices and  $10 \times 30 \text{ nm}^2$  for the FinFETs) were simulated as well and present the same characteristics as the  $5 \times 5 \text{ nm}^2$  and  $5 \times 15 \text{ nm}^2$  devices. Since the simulations are two-dimensional 2D, they represent long-channel devices.

The current is obtained by integrating the electron charge over the 2D device section at any gate voltage and multiplying it by a constant mobility and a small drain voltage. Mobility and drain voltage affect the current drive of the device, but not the subthreshold slope or the energy of the subbands. The subthreshold curve, defined as  $dV_G/d[\log(I_D)]$  plotted versus  $V_G$  is shown in Fig. 1 for the different devices, as a function of the average electron concentration. We define the subthreshold swing as the constant minimum value of the subthreshold curve before the curve takes off, i.e., typically for electron concentrations below  $10^{14} \text{ cm}^{-3}$ .

In the GAA device, the long-channel subthreshold swing reaches the theoretical limit of 59.6 mV/decade at  $T = 300 \text{ K}$  because there is no body effect in this device. This optimum subthreshold swing value is obtained regardless of the simulator used (classical or quantum), and regardless of the operation mode of the device (inversion or accumulation). In the FinFET, similar subthreshold swing values are obtained, whether classical (*P*) or quantum (*P+S*) simulations are used. The subthreshold swing value in the FinFET

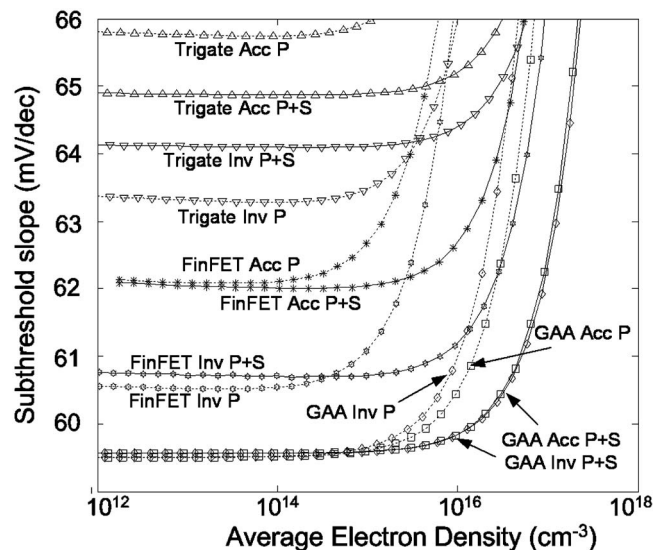


FIG. 1. Subthreshold swing in IM (Inv.) and AM (Acc.) trigate FETs calculated using the Poisson equation (*P*) or a Poisson/Schrödinger solver (*P+S*). The device has a long channel and is operated at low drain bias.

<sup>a)</sup>Electronic mail: jean-pierre.colinge@tyndall.ie.

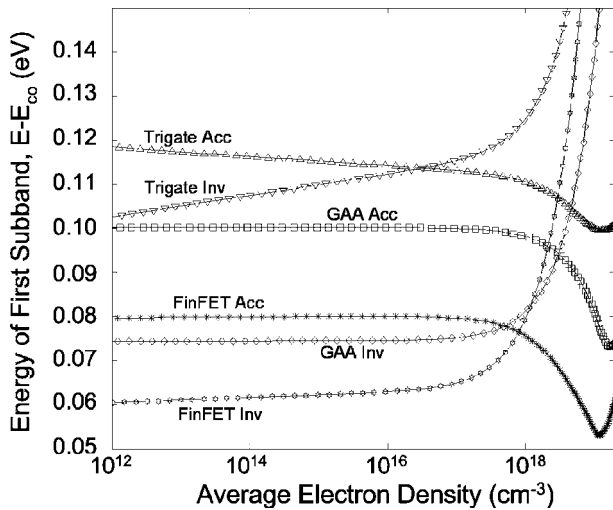


FIG. 2. Minimum energy of first subband vs average electron concentration in IM (Inv.) and AM (Acc.) trigate FETs calculated using the Poisson equation ( $P$ ) or a Poisson/Schrödinger solver ( $P+S$ ).

is a slightly higher than in the GAA device because there is a nonzero body effect. The swing in the AM FinFET is larger than that in the IM device because the charge centroid of the AM device is in the center of the devices (at a distance  $W_{Si}/2$  from the lateral Si/SiO<sub>2</sub> interfaces), while the charge centroids in the IM device are located at a smaller distance from the interfaces.<sup>7</sup> The subthreshold swing is larger in the trigate device than in the two other devices because of a larger body effect.<sup>8,9</sup> It is interesting to note that the classical simulation overestimates the value of subthreshold swing in the AM device, while it underestimates it in the IM device.

Figure 2 helps in understanding the discrepancy between the classical and quantum calculations in trigate devices. In the GAA device, where there is no back gate and, therefore, no body effect. The shape of the potential distribution within the silicon remains unchanged as long as the device is in subthreshold operation, i.e., when the electron concentration is too low to exert any significant influence on the charge term ( $\rho$ ) of Poisson's equation  $\nabla^2\Phi = -(\rho/\epsilon)$ . Since the shape of the potential distribution in the silicon does not change under these conditions, the minimum of the first energy subband stays constant as long as the electron concentration is below  $10^{17}$  cm<sup>-3</sup>. The energy is larger in the AM GAA device than in the IM GAA FET because the doping concentration is higher, which increases the depletion charge density and, hence, the electric field in the silicon. This increased electric field "squeezes" the electrons in a smaller area in the center of the device, which increases their energy. Mathematically, this is caused by the increase of the  $-(\hbar^2/2m)\nabla^2\Psi$  term in Schrödinger's equation. In other words, the increase or decrease of the energy level is related to the variation of the potential profile in the silicon, which causes a "compression" or "decompression" of the electron gas. At higher electron concentrations (above threshold), the energy level increases in the IM devices because the electrons are squeezed into a small fraction of the silicon near the silicon-gate oxide interfaces when the gate voltage is increased. This brings about a monotonic increase of the subband energy with gate voltage and electron concentration above threshold (Fig. 2). A different behavior is observed in the AM devices. In subthreshold operation, GAA and FinFET AM devices are fully depleted, and the shape of the

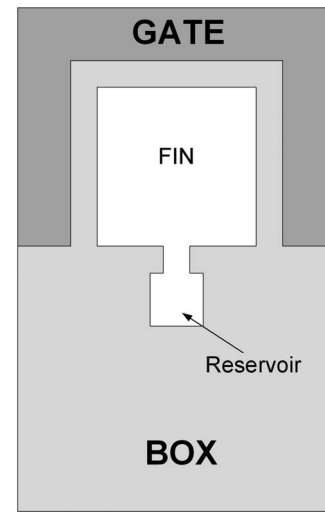


FIG. 3. AM multigate FET (MuGFET) with an electron reservoir below the fin.

potential in the silicon does not change. The subband energy remains constant when the gate voltage is increased. When the gate voltage reaches the body current threshold, a neutral zone is created near the center of the device, which increases in size when the gate voltage is increased. This allows the electron wave function to spread across the entire cross section of the device until flatband is reached (the electron gas is decompressed), and the subband energy decreases (for electron concentrations between  $10^{18}$  and  $10^{19}$  cm<sup>-3</sup> in Fig. 2). The energy reaches a minimum when the device is in flatband condition. Any further increase of gate voltage confines the electrons in surface channels, which increases their energy.

In the trigate device, a variation of the subband energy is observed in the subthreshold regime. In the IM trigate device in subthreshold operation, the minimum energy increases with gate voltage because the electron wave function is confined to an increasingly smaller region at the top of the device when  $V_G$  increases. In the AM trigate device, on the other hand, the wave function is initially confined to a small region at the bottom center of the device, and it spreads out to a larger fraction of the silicon as the gate voltage is increased, which decreases the electron energy. As a result, the minimum of the conduction band increases in the IM trigate device and decreases in the AM device as the gate voltage increases. This quantum effect improves the subthreshold swing in the AM FET and degrades it in the IM device, as compared to what classical simulation (Poisson only) predicts.

To further illustrate this phenomenon of subband energy variation with electron gas compression, we simulate a special structure with an electron "reservoir" below the silicon fin (Fig. 3). Such a device can be fabricated using multigate SOI MOSFET processing techniques.<sup>10,11</sup> The cross section of the fin itself is  $8 \times 8$  nm<sup>2</sup> while the dimensions of the reservoir are  $4 \times 4$  nm<sup>2</sup>. The reservoir is connected to the fin by a 4-nm-deep and 1.5-nm-wide silicon "tunnel." The gate oxide thickness is 2 nm and the BOX thickness is 20 nm. The device operates in accumulation mode and the acceptor doping concentration is  $N_d = 10^{18}$  cm<sup>-3</sup>. The gate material is chosen such that the flatband voltage  $V_{FB}$  is equal to 0.5 V.

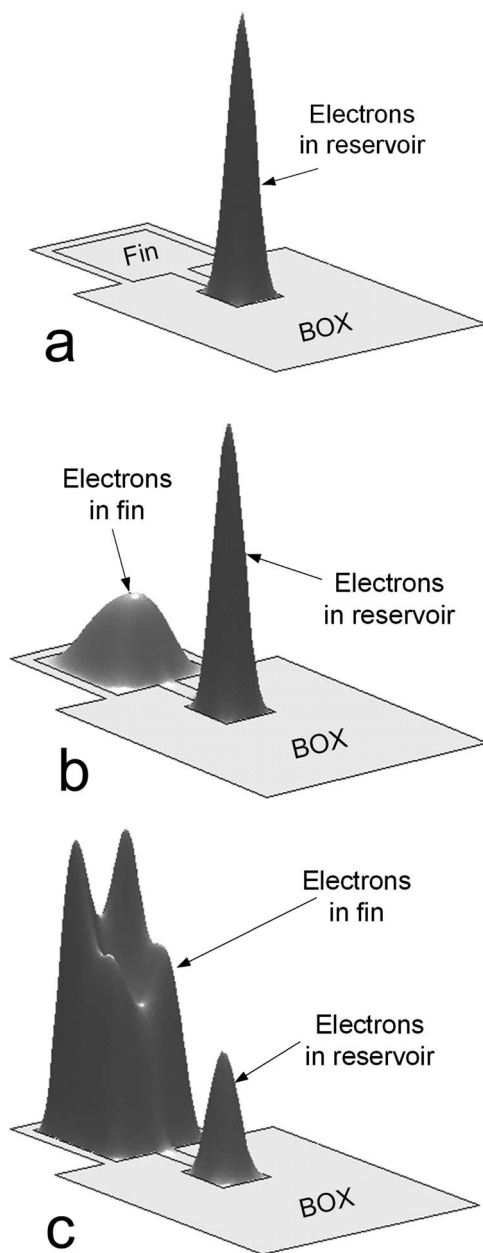


FIG. 4. Electron concentration at (a)  $V_G = -0.5$  V, (b)  $V_G = 0.3$  V, and (c)  $V_G = +0.9$  V in the AM MuGFET with an electron reservoir.

When a negative gate voltage is applied, the electrons are repelled by the gate and the electron wave functions are compressed in the small volume of the reservoir [Fig. 4(a),  $V_G = -0.5$  V], which creates relatively high subband energy levels, due to the small physical dimensions of the reservoir. As the gate voltage is increased, the electrons move “up” toward the fin, where they “decompress,” since the cross-sectional area of the fin is much larger than that of the reservoir [Fig. 4(b)]. As a result, and the energy values decrease (Fig. 5,  $V_G = 0$  V). At very high gate voltage, the wave functions are again “compressed” in two peaks near the top of the fin [Fig. 4(c),  $V_G = 0.9$  V], and the energy increases again (Fig. 5). The energy of the first subband is shown in Fig. 5 in the AM device with a reservoir, as a function of electron density. It decreases when the electron gas is decompressed and increases when it is compressed. The effect on this energy reduction on the subthreshold slope curve can be seen in Fig. 6, where the classical and quantum simulations are com-

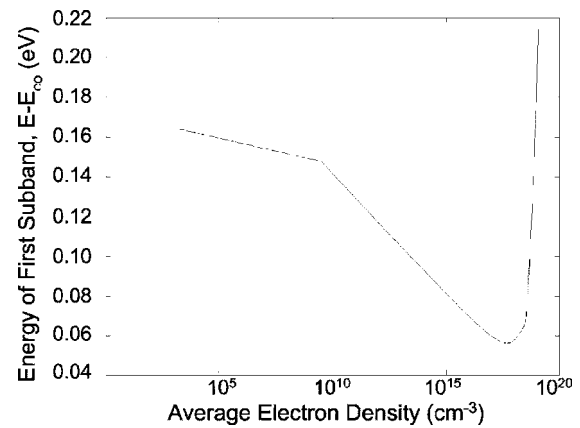


FIG. 5. Energy of first subband vs electron concentration in the AM MuGFET with an electron reservoir.

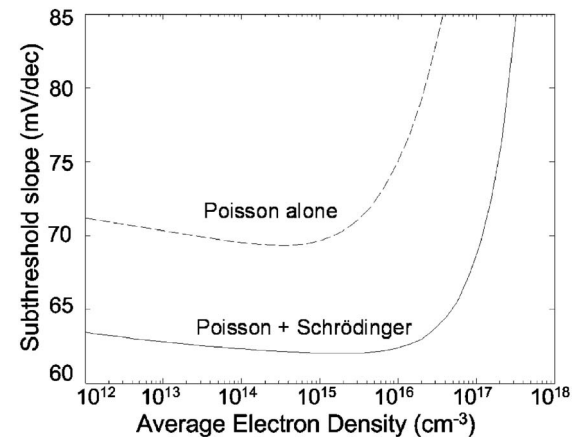


FIG. 6. Subthreshold curve vs electron concentration in the AM MuGFET with an electron reservoir.

pared. The subthreshold slope is significantly improved by the subband energy reduction that accompanies the decompression of the electron gas.

This material is based upon works supported by Science Foundation Ireland under Grant No. 05/IN/I888.

- <sup>1</sup>Y. Omura, S. Horiguchi, M. Tabe, and K. Kishi, *IEEE Electron Device Lett.* **14**, 569 (1993).
- <sup>2</sup>B. Majkusiak, T. Janik, and J. Walczak, *IEEE Trans. Electron Devices* **45**, 1127 (1998).
- <sup>3</sup>T. Poiroux, M. Vinet, O. Faynot, J. Widiez, J. Lolivier, T. Ernst, B. Previtali, and S. Deleonibus, *Microelectron. Eng.* **80**, 378 (2005).
- <sup>4</sup>K. Uchida, J. Koga, R. Ohba, T. Numata, and S. I. Takagi, *Tech. Dig. - Int. Electron Devices Meet.* **2001**, 29.4.1.
- <sup>5</sup>T. Ernst, D. Munteanu, S. Cristoloveanu, T. Ouisse, N. Hefyene, S. Horiguchi, Y. Ono, Y. Takahashi, and K. Murase, *Proceedings of the IEEE International SOI Conference, 1999*, p. 92.
- <sup>6</sup>J. P. Colinge, J. C. Alderman, W. Xiong, and C. R. Cleavelin, *IEEE Trans. Electron Devices* **53**, 1131 (2006).
- <sup>7</sup>J. P. Colinge, D. Flandre and F. Van de Wiele, *Solid-State Electron.* **37**, 289 (1994).
- <sup>8</sup>J. Frei, C. Johns, A. Vazquez, W. Xiong, C. R. Cleavelin, T. Schulz, N. Chaudhary, G. Gebara, J. R. Zaman, M. Gostkowski, K. Matthews, and J. P. Colinge, *IEEE Electron Device Lett.* **25**, p. 813 (2004).
- <sup>9</sup>M. Gaillardin, P. Paillet, V. Ferlet-Cavrois, O. Faynot, C. Jahan, and S. Cristoloveanu, *IEEE Trans. Nucl. Sci.* **53**, 3158 (2006).
- <sup>10</sup>X. Baie, X. Tang and J. P. Colinge, *Jpn. J. Appl. Phys., Part 1* **37**, 1591 (1998).
- <sup>11</sup>X. Tang, X. Baie, J. P. Colinge, A. Crahay, B. Katschmarskyj, V. Scheuren, D. Spöte, N. Reckinger, F. Van de Wiele, and V. Bayot, *Solid-State Electron.* **44**, 2259 (2000).